Inorg. Chem. **2008**, *47*, 2325−2333

Cobalt(II)/Nickel(II)-Centered Keggin-Type Heteropolymolybdates: Syntheses, Crystal Structures, Magnetic and Electrochemical Properties

Guang-Gang Gao, **Lin Xu**,* **Wen-Ju Wang**, **Xiao-Shu Qu**, **Hong Liu**, **and Yan-Yan Yang**

Key Laboratory of Polyoxometalate Science of Ministry of Education Institute of Polyoxometalate Chemistry, Department of Chemistry, Northeast Normal University, Changchun, Jilin 130024, People's Republic of China

Received April 26, 2007

New Keggin-type cobalt(II)/nickel(II)-centered heteropolymolybdates, $(C_3H_5N_2)_6[Co^{II}Mo_{12}O_{40}]\cdot 10H_2O$ (**1**) and $(NH_4)_3(C_4H_5N_2O_2)_3[Ni^{II}Mo_{12}O_{40}]$ (**2**), were isolated and characterized by IR, UV–vis, single-crystal X-ray diffraction, thermogravimetric, magnetic, as well as electrochemical analyses. The polyanion in the two compounds displays the well-known α-Keggin structure, which is composed of four Mo_3O_{13} units formed by edge-sharing octahedra. Four Mo_3O_{13} units connect each other by vertices, and the Co^{2+} or Ni^{2+} is located in the center. Magnetic measurements show that the central Co^{2+} and Ni^{2+} are in high spin states (with $S = {}^3/_2$ and $S = 1$, respectively) exhibiting paramagnetic behaviors. Cyclic voltammetric experiments for **1** represent a quasi-reversible one-electron redox Co^{3+}/Co^{2+} couple and two four-electron reversible redox processes ascribed to Mo centers, while **2** only shows two four-electron redox processes attributed to Mo centers in pH = 0.5 H_2SO_4 solution.

Introduction

Polyoxometalates (POMs), as a rich class of inorganic metal−oxide cluster compounds, have large numbers of structural diversity[1–8] and various applications in different areas, including optics,[9,10] magnetism,[11,12] catalysis,[13–17] medicine, and biology.[18,19] Keggin-type polyanions with highly symmetric structures are well-known as one kind of POMs since the first polyanion $[PMo_{12}O_{40}]^{3-}$ was reported by Berzelius in 1826 and then structurally determined by Keggin.[20–22] Up to now, Keggin-type compounds and their derivatives remain the most intriguing family in POM chemistry due to their robust structure and their interesting properties and possible applications in different fields such as catalysis,[23–31] materials science,[32–39] and medicine.[40] Their formula can be generally expressed as $[XM_{12}O_{40}]^{n-}$ (M =

* E-mail: linxu@nenu.edu.cn. Tel: +86-431-85099668.

(1) Liu, G.; Liu, T.; Mal, S. S.; Kortz, U. *J. Am. Chem. Soc.* **2006**, *128*, 10103–10110.
(2) Kasai, J.; Nakagawa, Y.; Uchida, S.; Yamaguchi, K.; Mizuno, N. *Chem.—Eur. J.* **2006**, *12*, 4176–4184.
(3) Liu, G.; Liu, T. *J. Am. Chem. Soc.* **2005**, *127*, 6942–6943.
(4) Kawamoto, R.; Uchida, S.; Mizuno, N. *J. Am. Chem. Soc.* **2005**, *127*, 10560–10567.
(5) Reinoso, S.; Vitoria, P.; Felices, L. S.; Lezama, L.; Gutiérrez-Zorrilla, J. M. *Chem.—Eur. J.* **2005**, *11*, 1538–1548.
(6) Bassil, B. S.; Nellutla, S.; Kortz, U.; Stowe, A. C.; Tol, J. V.; Dalal, N. S.; Keita, B.; Nadjo, L. *Inorg. Chem.* **2005**, *44*, 2659–2665.
(7) Mbomekalle, I. M.; Keita, B.; Nadjo, L.; Hardcastle, K. I.; Hill, C. L.; Anderson, T. M. *Dalton Trans.* **2004**, 4094–4095.
(8) Ritorto, M. D.; Anderson, T. M.; Neiwert, W. A.; Hill, C. L. *Inorg. Chem.* **2004**, *43*, 44–49.
(9) Ruether, T.; Hultgren, V. M.; Timko, B. P.; Bond, A. M.; Jackson, W. R.; Wedd, A. G. *J. Am. Chem. Soc.* **2003**, *125*, 10133–10143.
(10) Yamase, T.; Prokop, P. V. *Angew. Chem., Int. Ed.* **2002**, *41*, 466–469.
(11) Mialane, P.; Duboc, C.; Marrot, J.; Rivière, E.; Dolbecq, A.; Sécheresse, F. *Chem.—Eur. J.* **2006**, *12*, 1950–1959.
(12) Manos, M. J.; Tasiopoulos, A. J.; Tolis, E. J.; Lalioti, N.; Woollins, J. D.; Slawin, A. Z.; Sigalas, M. P.; Kabanos, T. A. *Chem.—Eur. J.* **2003**, *9*, 695–703.
(13) Boglio, C.; Lemière, G.; Hasenknopf, B.; Thorimbert, S.; Lacôte, E.; Malacria, M. *Angew. Chem., Int. Ed.* **2006**, *45*, 3324–3327.
(14) Khenkin, A. M.; Weiner, L.; Neumann, R. *J. Am. Chem. Soc.* **2005**, *127*, 9988–9989.
(15) Yin, C. X.; Finke, R. G. *J. Am. Chem. Soc.* **2005**, *127*, 9003–9013.
(16) Plault, L.; Hauseler, A.; Nlate, S.; Astruc, D.; Ruiz, J.; Gatard, S.; Neumann, R. *Angew. Chem., Int. Ed* **2004**, *43*, 2924–2928.
(17) Bar-Nahum, I.; Khenkin, A. M.; Neumann, R. *J. Am. Chem. Soc.* **2004**, *126*, 10236–10237.
(18) Pope, M. T.; Muller, A. *Angew. Chem., Int. Ed. Engl.* **1991**, *30*, 34–48.
(19) Witvrouw, M.; Weigold, H.; Pannecouque, C.; Schols, D.; Clercq, E. D.; Holan, G. *J. Med. Chem.* **2000**, *43*, 778–783.
(20) Berzelius, J. *Poggendorff's Ann. Phys.* **1826**, *6*, 369–371.
(21) Keggin, J. F. *Proc. R. Soc.* **1934**, *A144*, 75–100.
(22) Keggin, J. F. *Nature* **1933**, *131*, 908–909.
(23) Neumann, R. *Prog. Inorg. Chem.* **1998**, *47*, 317–370.
(24) Kozhevnikov, I. V. *Chem. Rev.* **1998**, *98*, 171–198.
(25) Hill, C. L.; Prosser-McCartha, C. M. *Coord. Chem. Rev.* **1995**, *143*, 407–455.
(26) Okuhara, T.; Mizuno, N.; Misono, M. *Appl. Catal., A* **2001**, *222*, 63–77.
(27) Mizuno, N.; Misono, M. *Chem. Rev.* **1998**, *98*, 199–217.
(28) Maayan, G.; Popovitz-Biro, R.; Neumann, R. *J. Am. Chem. Soc.* **2006**, *128*, 4968–4969.
(29) Neumann, R.; Khenkin, A. M. *Chem. Commun.* **2006**, 2529–2538.

10.1021/ic700797v CCC: $40.75
Published on Web 02/23/2008

W, Mo; X = P, Si, B, Ge, As, S, Al,[41–43] Co, Fe, Cu, V, Zn[44–47]). Among these species, the most studies are focused on main-group atom-centered polyoxoanions, while the transition-metal-centered Keggin-type compounds are rarely explored.[47] Especially, transition metal cations inserted within the Keggin structure are rare indeed but not in the Anderson structure. In 1999, an isopolyoxomolybdate anion, $[Mo_{0.5}Mo_{12}O_{40}]^{6-}$, was characterized by Duraisamy et al.[48] This β-Keggin-type $[Mo_{0.5}Mo_{12}O_{40}]^{6-}$ polyanion accommodates a central MoO_4 tetrahedron, suggesting the feasibility of new Keggin-type species with a centered transition metal ion. However, the predominant Mo anions in different acidic solutions are isopolymolybdates such as heptamolybdate, $(H_nMo_7O_{24})^{6-n}$, $n \leq 3$, and octamolybdates, $(H_nMo_8O_{26})^{4-n}$, $n \leq 1$, and $(H_nMo_8O_{28})^{8-n}$, $1 \leq n \leq 3$.[49–51] These dominating components hinder the self-assembly of the dodecamolybdate framework. It remains a challenge in the synthesis of transition-metal-centered Keggin-type heteropolymolybdates. Inspired by the syntheses of $[Co^{II}W_{12}O_{40}]^{6-}$ and $[Ni_4(H_2O)_2(\alpha\text{-}NiW_9)_2]^{16-}$ polyanions,[52–55] we make an effort to isolate Co^{2+}- or Ni^{2+}-centered Keggin heteropolymolybdate. By a large number of experiments, new α-Keggin-type species, $(C_3H_5N_2)_6[Co^{II}Mo_{12}O_{40}]\cdot 10H_2O$ (**1**) and $(NH_4)_3(C_4H_5N_2O_2)_3[Ni^{II}Mo_{12}O_{40}]$ (**2**), were successfully synthesized under conventional and hydrothermal conditions, respectively. Herein, we report the syntheses, crystal structures, thermogravimetric, magnetic, and electrochemical properties. The successful isolation and structural characterization of the two compounds are of the following significance. First, the introduced Co^{2+}/Ni^{2+} could modify the physicochemical properties of **1** or **2** due to the centered Co^{2+}/Ni^{2+} with 3d electrons being different than other centered main group elements. Second, these new polyanions could be further tailored to become lacunary derivatives or functionalization by other organic or inorganic groups, resulting in a new series of fascinating hybrid materials. Third, the Co^{2+}/Ni^{2+} could affect the electrochemical properties ascribed to shell Mo centers. Thus **1** and **2** are possibly used in electrochemical catalysis.

Experimental Section

Syntheses. All chemicals were used as purchased. Distilled water was used throughout. $K_6CoW_{12}O_{40}\cdot 16H_2O$ (CoW_{12})[52] and $H_4SiMo_{12}O_{40}\cdot 15H_2O$ ($SiMo_{12}$)[56] were synthesized according to the literature methods.

$(C_3H_5N_2)_6[Co^{II}Mo_{12}O_{40}]\cdot 10H_2O$ (1). $Na_2MoO_4\cdot 2H_2O$ (1.245g, 5 mmol) and CH_3COONa (0.5 g, 6 mmol) were dissolved in 20 mL of distilled water followed by addition of 0.238 g (0.83 mmol) of $Co(CH_3COO)_2\cdot 4H_2O$. The solution was stirred for 10 min, and 0.225 g (3.3 mmol) of imidazole was added. Then the pH value was adjusted to about 4.6–4.8 by 85% acetic acid to form a deep red solution. The solution was stirred and refluxed at 55–60 °C in glass flask for about 3 hours then was allowed to cool to room temperature and filtered into a 50 mL beaker (final pH still in the range of 4.6–4.8). Several days later, brown plate crystals of **1** (yield ca. 6%; all yields were calculated based on Mo) formed by evaporating the solution at room temperature, which could be collected and suitable for X-ray diffraction. The small portion of white and light yellow powders were unidentified. Without the addition of CH_3COONa, **1** can also be formed but with a very low yield (ca. 0.5% based on Mo). We also found that the other Co/Mo molar ratio as either smaller or larger than 1:6 all led to low yield. Anal. Calcd for **1**, $C_{18}H_{50}N_{12}CoMo_{12}O_{50}$: Co, 2.41; Mo, 47.09; C, 8.84; H, 2.06; N, 6.87%. Found: Co, 2.38; Mo, 46.95; C, 8.76; H, 1.93; N, 6.79%. IR (KBr, cm^{-1}): 3430, 3107, 2805, 2599, 1572, 1419, 1173, 1087, 963, 874, 795, 620, 460 (Figure S1, top).

$Na_4[Mo_8O_{27}Co(H_2O)_4]\cdot 16H_2O$ (Mo_8Co). The synthetic procedure is similar to that of **1** except that no imidazole was added and the reaction pH was adjusted to 3.0. Two weeks later, pink crystals of Mo_8Co formed with a yield 26%. Anal. Calcd for $H_{40}O_{47}Na_4CoMo_8$: Co, 3.45; Mo, 44.87%. Found: Co, 3.36; Mo, 44.78%. IR (KBr, cm^{-1}): 3419 (s), 1627 (m), 938 (s), 913 (s), 892 (s), 853 (m), 703 (s), 658 (s), 560 (s) (Figure S2, top).

$(C_3H_5N_2)_4[Co(H_2O)_5Mo_7O_{24}]\cdot 6H_2O$ (Mo_7Co). The synthetic procedure is the same as that of **1**. After no products of **1** formed, all of the solid products in the mother liquor were removed by filtration. The filtrate was added to additional water (~20%) and then the solvent was allowed to evaporate at room temperature (pH ≈ 4.9). After 2 weeks, pink crystals of Mo_7Co formed with a yield of 33%. Anal. Calcd for $H_{42}C_{12}N_8O_{35}CoMo_7$: Co, 3.71; Mo, 42.26%. Found: Co, 3.60; Mo, 42.35%. IR (KBr, cm^{-1}): 3467, 3140, 2975, 2837, 2623, 1581, 1424, 1313, 1170, 1084, 936, 898,

(30) Maayan, G.; Ganchegui, B.; Leitner, W.; Neumann, R. *Chem. Commun.* **2006**, 2230–2232.
(31) Nagarapu, L.; Apuri, S.; Kantevari, S. *J. Mol. Catal. A* **2006**, *266*, 104–108.
(32) Lapkin, A.; Savill-Jowitt, C.; Edler, K.; Brown, R. *Langmuir* **2006**, *22*, 7664–7671.
(33) Gamelas, J. A. F.; Santos, F. M.; Felix, V.; Cavaleiro, A. M. V.; de Matos Gomes, E.; Belsley, M.; Drew, M. G. B. *Dalton Trans.* **2006**, 1197–1203.
(34) Sanyal, A.; Mandal, S.; Sastry, M. *Adv. Funct. Mater.* **2005**, *15*, 273–280.
(35) Coronado, E.; Day, P. *Chem. Rev.* **2004**, *104*, 5419–5448.
(36) Gomez-Romero, P. *Adv. Mater.* **2001**, *13*, 163–174.
(37) Clemente-Juan, J. M.; Coronado, E. *Coord. Chem. Rev.* **1999**, *193–195*, 361–394.
(38) Coronado, E.; Gomez-Garcia, C. J. *Chem. Rev.* **1998**, *98*, 273–296.
(39) Ouahab, L. *Coord. Chem. Rev.* **1998**, *178–180*, 1501–1531.
(40) Rhule, J. T.; Hill, C. L.; Judd, D. A. *Chem. Rev.* **1998**, *98*, 327–357.
(41) Pope, M. T. *Heteropoly and Isopoly Oxometalates*; Springer: Berlin, 1983.
(42) Weinstock, I. A.; Cowan, J. J.; Barbuzzi, E. M. G.; Zeng, H.; Hill, C. L. *J. Am. Chem. Soc.* **1999**, *121*, 4608–4617.
(43) Himeno, S.; Miyashita, K.; Saito, A.; Hori, T. *Chem. Lett.* **1990**, 799–802.
(44) Casañ-Pastor, N.; Gonez-Romero, P.; Jamesson, G. B.; Baker, L. C. W. *J. Am. Chem. Soc.* **1991**, *113*, 5658–5663.
(45) Khan, M. I.; Cevik, S.; Hayashi, R. *J. Chem. Soc., Dalton Trans.* **1999**, 1651–1654.
(46) Gómez-García, C. J.; Giménez-Saiz, C.; Triki, S.; Coronado, E.; Magueres, P. L.; Quahab, L.; Ducasse, L.; Sourisseau, C.; Delhaes, P. *Inorg. Chem.* **1995**, *34*, 4139–4151.
(47) Niu, J. Y.; Wang, Z. L.; Wang, J. P. *Inorg. Chem. Commun.* **2003**, *6*, 1272–1274.
(48) Duraisamy, T.; Ramanan, A.; Vittal, J. J. *J. Mater. Chem.* **1999**, *9*, 763–767.
(49) Müller, A.; Peter, F. *Chem. Rev.* **1998**, *98*, 239–271.
(50) Bal, Y.; Bal, K-E.; Cotè, G.; Lallam, A. *Hydrometallurgy* **2004**, *75*, 123–124.
(51) Coué, V.; Dessapt, R.; Bujoli-Doeuff, M.; Evain, M.; Jobic, S. *Inorg. Chem.* **2007**, *46*, 2824–2835.
(52) Matsumoto, M.; Neuman, N. I.; Swaddle, T. W. *Inorg. Chem.* **2004**, *43*, 1153–1158.
(53) Baker, L. C. W.; McCutcheon, T. P. *J. Am. Chem. Soc.* **1956**, *78*, 4503–4510.
(54) Acerete, R.; Casan-Pastor, N.; Bas-Serra, J.; Baker, L. C. W. *J. Am. Chem. Soc.* **1989**, *111*, 6049–6056.
(55) Wang, J. P.; Ma, P. T.; Shen, Y.; Niu, J. Y. *Cryst. Growth Des.* **2007**, *4*, 603–605.
(56) Tsigdinos, G. A. *Ind. Eng. Chem., Prod. Res. Dev.* **1974**, *13*, 267–274.

830, 751, 663, 545 (Figure S2, bottom). Crystal data in CIF format, selected bond lengths and angles, description of the structures, and structural figures of complexes Mo_8Co and Mo_7Co are given in Supporting Information.

$(NH_4)_3(C_4H_5N_2O_2)_3NiMo_{12}O_{40}$ (2). A mixture of MoO_3 (8 mmol), $NiCl_2{\cdot}6H_2O$ (0.5 mmol), 4,5-imidazoledicarboxylic acid (0.75 mmol), CH_3COONH_4 (2 mmol), and water (8 mL) in the molar ratio of 16:1:1.5:4:889 was sealed in a 15 mL Teflon-lined stainless container and heated at 140 °C for 7 days under autogenous pressure. After cooling to room temperature, dark green single crystals of **2** were obtained in 18% yield based on Mo. Anal. Calcd for $C_{12}H_{27}NiMo_{12}N_9O_{46}$: Ni, 2.62; Mo, 51.32; C, 6.24; H, 1.21; N, 5.62%. Found: Ni, 2.54; Mo, 51.21; C, 6.12; H, 1.11; N, 5.50%. IR (KBr, cm^{-1}): 3550, 3160, 2876, 1726, 1591, 1487, 1427, 1315, 1180, 1083, 968, 882, 800, 624, 467 (Figure S1, bottom). It should be noteworthy that the powder samples of **2** (obtained from single crystals being crushed with an agate mortar) show lower solubility in pH < 0 acidic solution. When these powder samples were dissolved in pH < 0 H_2SO_4 media under stirring for more than 15 min, the color of the mixture changed from green to blue, indicating the presence of reduced polyanions $[NiMo_{12}O_{40}]^{x-}$ ($x > 6$). The increase of the reduced species of **2** in pH < 0 solution possibly leads to the lower solubility.

Elemental analyses (C, H, N) were performed with a Perkin-Elmer 2400 CHN elemental analyzer; Co and Mo were analyzed with a PLASMA-SPEC(I) ICP atomic emission spectrometer. IR spectra were recorded on a BRUKER Vertex 70 FT/IR spectrophotometer using KBr pellets. TGA analysis was conducted on Perkin-Elmer TGA7 equipment under nitrogen with a heating of 5 °C min^{-1} from 30 to 800 °C. The X-ray photoelectron spectra (XPS) were recorded on a USWHA150 photoelectron spectroscope using monochromatic Al Kα (1486.6 eV) radiation.

X-ray Crystallography. Single-crystal data of **1** and **2** were collected on a Bruker SMART APEX II CCD single-crystal diffractometer using Mo Kα radiation ($\lambda = 0.71073$ Å). Direct methods were used to solve the structure and to determine the molybdenum, cobalt, and nickel atoms (SHELXS-97).[57] The other atoms were found from successive difference maps (SHELXL-97). All the H atoms that belong to organic molecules were placed at calculated positions and were allowed to ride on the carrier atoms with $U_{iso} = 1.2U_{eq}$. All of the other H atoms that belong to water or ammonium molecules were not determined. All of the non-hydrogen atoms were refined anisotropically. Absorption corrections were performed using the SADABS propgram.[58] Crystallographic data are summarized in Table 1.

UV–Vis Spectroscopy. All reagents were used as purchased. Pure water was used throughout by a Millipore-Q Academic purification set. The UV–vis spectra were recorded on a HITACHI UV-3010 spectrophotometer. The 1.00 cm optical-path quartz cuvettes (Shanghai Optical Instrument Company, China) were used. The different pH values of the media were adjusted by 3 M H_2SO_4.

Magnetic Properties. Variable-temperature susceptibility measurements were carried out on a single-crystal sample of **1** or **2** in the temperature range of 2–300 K at a magnetic field of 10 kOe with a magnetometer (Quantum Design MPMSXL-5) equipped with a SQUID sensor. The diamagnetic correction of susceptibility data was carried out by means of Pascal's constants.[59]

Electrochemical Experiments. The electrochemical properties were performed on a CHI 660 Electrochemical workstation (USA) for control of the electrochemical measurements and for data collection. A conventional three-electrode system was used to investigate the cyclic voltammetric behaviors. The glass carbon electrode was used as a working electrode, Ag/AgCl (3 mol/L KCl) as a reference electrode, Pt coil as a counter electrode, and the 2 M H_2SO_4 or H_2SO_4 solutions with different pH values were used as electrolytes. The concentrations of **1**, **2**, $SiMo_{12}$, and CoW_{12} in the measurement of cyclic voltammetric behaviors were all 1.0×10^{-3} M. The solutions were deaerated for at least 20 min with pure nitrogen and a small nitrogen flow was kept above the liquid face during the experiments.

Table 1. Crystal Data and Structure Refinement for **1** and **2**

compound	**1**	**2**
empirical formula	$C_{18}H_{50}CoMo_{12}N_{12}O_{50}$	$C_{12}H_{27}NiMo_{12}N_9O_{46}$
formula weight	2444.85 g·mol^{-1}	2243.35 g·mol^{-1}
temperature	185(2) K	293(2) K
wavelength	0.71073 Å	0.71073 Å
crystal system	orthorhombic	trigonal
space group	*Fmmm*	$R\bar{3}$
unit cell dimensions	$a = 13.043(2)$ Å	$a = 17.972(2)$
	$b = 21.364(3)$ Å	$b = 17.972(2)$
	$c = 21.676(3)$ Å	$c = 24.263(3)$
	$\alpha = 90°$	$\alpha = 90°$
	$\beta = 90°$	$\beta = 90°$
	$\gamma = 90°$	$\gamma = 120°$
volume	6040.0(15) $Å^3$	6786.8(14) $Å^3$
Z, calculated density	4, 2.737 g/cm^3	3, 3.245 g/cm^3
$F(000)$	4740	6237
crystal size (mm^3)	0.204 × 0.193 × 0.112	0.242 × 0.181 × 0.135
limiting indices	$-16 \le h \le 7$	$-21 \le h \le 21$
	$-26 \le k \le 26$	$-19 \le k \le 21$
	$-26 \le l \le 26$	$-19 \le l \le 29$
data collected/unique	7468/1632	12136/2795
	[R(int) = 0.0828]	[R(int) = 0.0209]
completeness	98.6%	98.4%
refinement method	F^2	F^2
data/restraints/parameters	1632/0/135	2795/6/242
goodness of fit on F^2	0.957	1.015
final R indices [$I > 2\sigma(I)$]	$R = 0.0590$, $R_w = 0.1264$	$R = 0.0688$, $R_w = 0.1298$
R indices (all data)[a]	$R = 0.1114$, $R_w = 0.1440$	$R = 0.0743$, $R_w = 0.1452$
extinction coefficient	0.00038(7)	0.00014(3)
largest diff. peak and hole	1.180 and −1.148 e · $Å^{-3}$	1.316 and −1.186 e · $Å^{-3}$

[a] $R = \Sigma||F_o| - |F_c||/\Sigma|F_o|$. $R_w = \Sigma[w(F_o^2 - F_c^2)^2]/\Sigma[w(F_o^2)^2]^{1/2}$.

Results and Discussion

Synthesis. On the basis of the synthetic methods of $[Co^{II}W_{12}O_{40}]^{6-}$ and $[Mo_{0.5}Mo_{12}O_{40}]^{6-}$ polyanions,[48,52–54], we have tried to obtain **1** in the pH < 3.5 acidic solutions by reaction of $Na_2MoO_4{\cdot}2H_2O$ with $Co(CH_3COO)_2{\cdot}4H_2O$ directly or by additional organic cations. Unfortunately, all trials led to no anticipated products. Consequently, by the reaction of $Co(CH_3COO)_2{\cdot}4H_2O$, $Na_2MoO_4{\cdot}2H_2O$, and imidazole (molar ratio 1:6 for Co/Mo) at pH 4.6–4.8, brown crystals of **1** were isolated with a low yield (0.5%). The higher yield (6%) products were obtained by addition of CH_3COONa into the reaction system. In exact stoichiometric conditions, there were also low yield (2%) products formed. Therefore, the excessive $Co(CH_3COO)_2{\cdot}4H_2O$ and the buffer medium are key factors for obtaining high yield products. The tetramethylammoniumchloride and tetraethylammoniumchloride were also used to isolate the $[Co^{II}Mo_{12}O_{40}]^{6-}$ anion; however, brown polycrystalline or powder products formed. Moreover, without addition of imidazole (at pH = 3.0), there was only a crystalline complex Mo_8Co formed. So, the imidazole is a more suitable ligand for the isolation

(57) *SHELXTL*, version 5.1; Bruker AXS: Madison, WI, 1998.
(58) *SAINT*, version 6.02; Bruker AXS: Madison, WI, 1999.
(59) O'Conner, C. J. *Prog. Inorg. Chem.* **1982**, *29*, 203–283.

Scheme 1

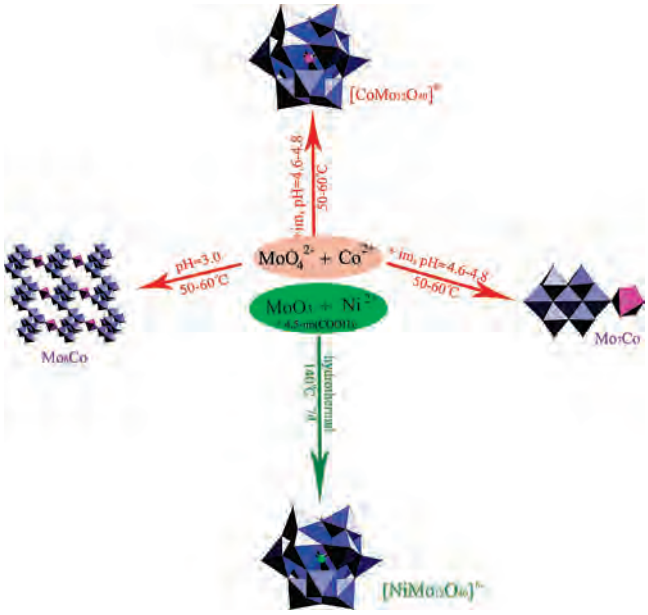

of **1**. After removing of solid products in the mother liquor of complex **1**, another polymolybdate Mo_7Co was obtained with a high yield of about 33%. This result confirmed that only a small portion of $[Co^{II}Mo_{12}O_{40}]^{6-}$ anions formed in the reaction. However, due to its more negative charge than the coexisting $[Mo_7O_{24}Co(H_2O)_5]^{4-}$ polyanion, $[Co^{II}Mo_{12}O_{40}]^{6-}$ can still be crystallized by imidazolium in a low yield. All these results reflect that **1** can be synthesized in weak acidic solution. The pH value, suitable organic cation, and excessive $Co(CH_3COO)_2{\cdot}4H_2O$ play key roles in the preparation of **1**. The complexes of Mo_8Co and Mo_7Co with higher yield are in agreement with the fact that $[Mo_7O_{24}]^{6-}$ anion is the predominant species in a pH range of 4.0–7.0, and only small portion MoO_4^{2-} anions are devoted to forming dodecamolybdate framework by self-assembly.[51]

When we tried to obtain other transition-metal-centered Keggin polyanions, the above approach failed. Therefore, we changed our strategy to synthesize such Keggin compounds under the hydrothermal conditions. The treatment of a mixture of MoO_3, $NiCl_6{\cdot}6H_2O$, 4,5-imidazoledicarboxylic acid, CH_3COONH_4, and distilled water in a 15 mL Teflon-lined stainless autoclave resulted in dark green single crystals of **2**. Interestingly, the starting material of 4,5-imidazoledicarboxylic acid transformed into protonated 5-imidazolecarboxylic acid in the final product, suggesting a decarboxylation in the reaction system. Furthermore, in the same conditions, if 4,5-imidazoledicarboxylic acid is replaced by imidazole, compound **2** cannot be obtained. These results indicate that the introduction of 4,5-imidazoledicarboxylic acid is a key factor to isolate **2** by hydrothermal method. The syntheses of the above complexes are shown in Scheme 1.

IR and UV–Vis Spectra. The IR spectra of the two compounds share similarly characteristic vibrational features to other Keggin structures[60] as shown in Figure S1. Symmetric and asymmetric stretching of the different Mo−O bonds are observed as follows: 963 cm^{-1} (**1**) and 968 cm^{-1} (**2**) for terminal Mo−O_t; 874 cm^{-1} (**1**) and 882 cm^{-1} (**2**) for Mo−O_b (O_b interbridges between corner-sharing octahedra); 795 cm^{-1} (**1**) and 800 cm^{-1} (**2**) for Mo−O_c (O_c intrabridges between edge-sharing octahedra); 620 cm^{-1} (**1**) and 624 cm^{-1} (**2**) bands are ascribed to the antisymmetric stretching vibrations of Mo−O_b and Mo−O_c, respectively. Bands at 3430, 3107, 2935, 2805, 2599, 1572, 1419, 1173, and 1087 cm^{-1} determine the presence of characteristic vibrational features of imidazole and water molecules in **1**, while bands at 3550, 3160, 2876, 1726, 1591, 1487, 1427, 1315, 1180, and 1083 cm^{-1} confirm the existence of 5-imidazolecarboxylic acid and ammonium molecules in **2**. The Co−O and Ni−O bands were also observed at 460 and 467 cm^{-1}, respectively.

Figure S5 shows the electronic spectra of **1** and **2** in the range from 200 to 400 nm. The plots contain two characteristic bands for the ligand-to-metal charge transfer in the polyanions. The more intense bands corresponding to the p_π (O_d) → d_{π^*} (Mo) transitions are centered at 205 nm (for **1**) and 208 nm (for **2**). The shoulder bands at 306 nm (for **1**) and 310 nm (for **2**) are assigned to the p_π ($O_{b,c}$) → d_{π^*} (Mo) charge transfer transition in the tricentric bonds. These values are close to the other Keggin anions.[61] The stabilities of **1** and **2** were further investigated in different pH solutions. The characteristic bands do not change notably within 72 h, indicating their stabilities in a broad pH range. Among the known Keggin-type heteropolymolybdate, **1** and **2** are more stable species than the others, such as 12-molybdophosphate which is generally labile in the pH > 4 aqueous solution.[62] In the visible region, **1** shows two bands at 575 and 645 nm ascribed to d−d transitions of tetrahedral Co^{2+} as shown in Figure S6. Though the expected band of d−d transition from the ground state $^4A_2(F)$ to the $^4T_1(P)$ state should be around 600 nm, the spin–orbit coupling causes the splitting of this band into two.[63] The greenish brown color of the sample solution also indicates a difference from the red-pink color (~515 nm) of the hexaaqua $[Co(OH_2)_6]^{2+}$ complex with an octahedral Co^{2+}.[64] For the deep green sample solution of **2**, two bands at 605 and 650 nm are assigned to the transition from the $^3T_1(^3F)$ ground state of Ni^{2+} in a tetrahedral site to the $^3T_1(^3P)$ excited state. The splitting is also due to the spin–orbit coupling. Similar absorption bands have been observed for the Ni^{2+}-doped $Ca_3Sc_2Ge_3O_{12}$ complex containing a tetrahedral $[NiO_4]$ group.[65]

Crystal Structures. The structure of **1** is composed of $[Co^{II}Mo_{12}O_{40}]^{6-}$ polyanion, imidazolium cations, and isolated

(60) Rocchiccioli-Deltcheff, C.; Fournier, M.; Frank, M.; Thouvenot, R. *Inorg. Chem.* **1983**, *22*, 207–216.
(61) Fruchart, J. M.; Herve, G.; Launay, J. P.; Massart, R. *J. Inorg. Nucl. Chem.* **1976**, *38*, 1627–1634.
(62) Gaunt, A. J.; May, I.; Sarsfield, M. J.; Collison, D.; Helliwell, M.; Denniss, I. S. *Dalton Trans.* **2003**, 2767–2771.
(63) Duan, X. L.; Yuan, D. R.; Cheng, X. F.; Wang, X. Q.; Wang, Z. M.; Xu, D.; Lv, M. K. *Opt. Mater.* **2003**, *23*, 327–330.
(64) Orgel, L. E. *An Introduction to Transition-Metal Chemistry: Ligand-Field Theory*; Butler & Turner Ltd.: London, 1966.
(65) Zannoni, E.; Cavalli, E.; Toncelli, A.; Tonelli, M.; Bettinelli, M. *J. Phys. Chem. Solids* **1999**, *60*, 449–455.

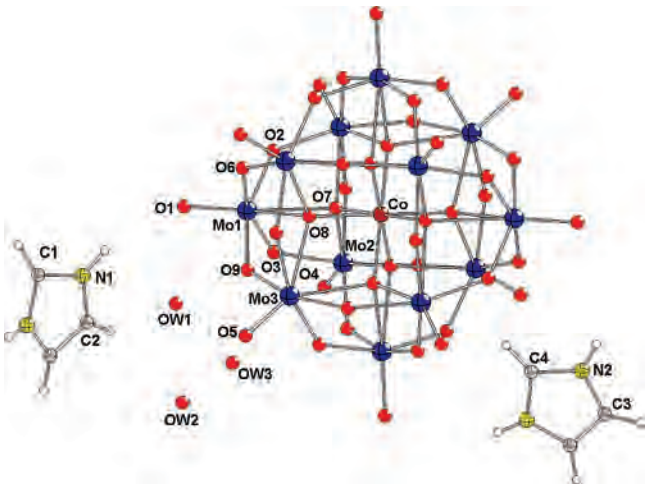

Figure 1. Ball-and-stick representation of **1** (asymmetric atom labels are shown).

water molecules as shown in Figure 1. This α-Keggin anion, $[Co^{II}Mo_{12}O_{40}]^{6-}$, is constructed of four Mo_3O_{13} units that are formed by edge-sharing MoO_6 octahedra, and they are linked to each other by vertices. The central cavity accommodates a Co^{2+} ion. However, the central four μ_4 oxygen atoms are observed to be disordered over eight positions, a usual problem for POM clusters.[46,66] We have collected single-crystal data three times by using different crystals; unfortunately, all data had the same problem. Nevertheless, both the chemical rationality of the Keggin structure and magnetic results are indicative of a CoO_4 coordination environment. There are three 2-fold rotation axes, three mirrors, and one inversion center. Co^{2+} is in the inversion center. Three 2-fold rotation axes pass through the central Co^{2+} along *a*, *b*, and *c* axes. The Co, O(5), O(6), O(8), Mo(3); Co, O(2), O(4), O(7), Mo(2); and Co, O(4), O(5), Mo(2), Mo(3) atoms are in three mirrors along [0 0 1], [1 0 0], and [0 1 0] direction. The longest Mo(1)−Mo(1), Mo(2)−Mo(2), and Mo(3)−Mo(3) distances are different as 7.085, 6.939, and 6.933 Å, which indicates the deviation from the high *Td* symmetry. The $Mo-O_t$, $Mo-O_b$, and $Mo-O_c$ distances are in the range of 1.67−1.72, 1.84−1.94, and 2.11−2.29 Å, respectively. These values are similar to other Keggin polyanions.[67–69] Selected bond lengths and angles are listed in Table S1. The average Co−O distance is 1.910 Å, a little longer than 1.895 Å in the $[Co^{II}W_{12}O_{40}]^{6-}$ polyanion.[44] Bond-valence sum calculations yielded values[70] of 5.85–6.15 for the Mo atoms and 2.20 for Co, close to the expected values of 6 and 2, respectively. This result is further confirmed by the X-ray photoelectron spectra (XPS). As shown in Figure 2, the Mo $3d_{5/2}$ and Co $2p_{3/2}$ binding energies are 232.6 and 781.0 eV,

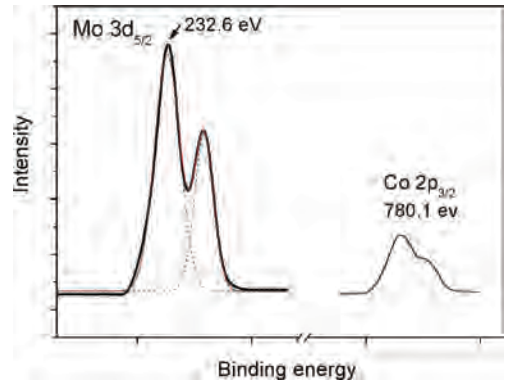

Figure 2. XPS spectra of **1** for Mo $3d_{5/2}$ and Co $2p_{3/2}$.

respectively, in agreement with the Mo^{6+} and Co^{2+} ions.[71–73] The semiquantitative elemental analysis also indicates the presence Co and Mo in the molar ratio of 1:12.03.

Two kinds of imidazolium cations are demonstrated. One (defined here as imi(1)) has a 2-fold rotation axis passing though the C(1) atom, and the other (defined here as imi(2)) has a 2-fold rotation axis passing through the C(4) atom and a mirror along the molecular plane. In the three-dimensional packing diagram, as shown in Figure S7 (top), the distances of Ow(2)−O5, Ow(3)−O9, C(1)−O2, and C(4)−O6 are 2.870, 2.978, 2.928, and 3.011 Å, respectively. These indicate that the hydrogen bonding interactions possibly exist among water molecules, imidazolium cations, and polyanions with contribution to the stability of the three-dimensional framework. The neighboring imi(2) cations are located in the same plane and extend as a zigzag way along the *a* axis, while the imi(1) cations propagate as face-to-face pairs along a 2-fold rotation axis.

The structure of **2** is composed of the $[Ni^{II}Mo_{12}O_{40}]^{6-}$ anion, protonated 5-imidazolecarboxylic acid, and ammonium cations, as shown in Figure 3. Though the $[Ni^{II}Mo_{12}O_{40}]^{6-}$ is isostructural to $[Co^{II}Mo_{12}O_{40}]^{6-}$ anion, it displays α-Keggin structure with a C_{3v} symmetry. There is a 3-fold rotation axis passing through the O(3) and Ni atoms. The central NiO_4 group shows a distorted tetrahedron with Ni−O distances in the range of 1.833(8)−1.844(9) Å. The $Mo-O_t$, $Mo-O_b$, and $Mo-O_c$ distances are similar to those in **1** (Table S1). Bond-valence sum calculations yielded values of 5.95–6.09 for the Mo atoms and 2.39 for Ni, close to the expected values of 6 and 2, respectively. This result is further confirmed by the X-ray photoelectron spectra. As shown in Figure 4, the Mo $3d_{5/2}$ and Ni $2p_{3/2}$ binding energies are 232.7 and 854.0 eV, respectively, in agreement with the Mo^{6+} and Ni^{2+} ions.[74] The semiquantitative elemental analysis also gives the presence of Ni and Mo in the molar ratio of 1:11.83. The 5-imidazolecarboxylic acid ligands in **2** not only act as organic cations but also link polyoxoanions by hydrogen bonding interactions (N—H···O or O—H···O)

(66) Balula, M. S. S.; Santos, I. C. M. S.; Gamelas, J. A. F.; Cavaleiro, A. M. V.; Binsted, N.; Schlindwein, W. *Eur. J. Inorg. Chem.* **2007**, 1027–1038.
(67) Chen, Q.; Hill, C. L. *Inorg. Chem.* **1996**, *35*, 2403–2405.
(68) Borrows, J. N.; Jameson, G. B.; Pope, M. T. *J. Am. Chem. Soc.* **1985**, *107*, 1771–1773.
(69) Chae, H. K.; Klemperer, W. G.; Laez Loyo, D.; Day, V. W.; Eberspacher, T. *Inorg. Chem.* **1992**, *31*, 3187–3189.
(70) Brown, I. D.; Altermatt, D. *Acta Crystallogr., Sect. B* **1985**, *41*, 244–247.
(71) Zhang, G. J.; Chen, Z. H.; He, T.; Ke, H. H.; Ma, Y.; Shao, K.; Yang, W. S.; Yao, J. N. *J. Phys. Chem. B* **2004**, *108*, 6944–6948.
(72) McIntyre, N. S.; Johnston, D. D.; Coatsworth, L. L.; Davidson, R. D.; Brown, J. R. *Surf. Interface Anal.* **1990**, *15*, 265–272.
(73) Bessel, C. A.; Rolison, D. R. *J. Phys. Chem. B* **1997**, *101*, 1148–1157.
(74) Hartman, J. R.; Combariza, M. Y.; Vachet, R. W. *Inorg. Chim. Acta* **2004**, *357*, 51–58.

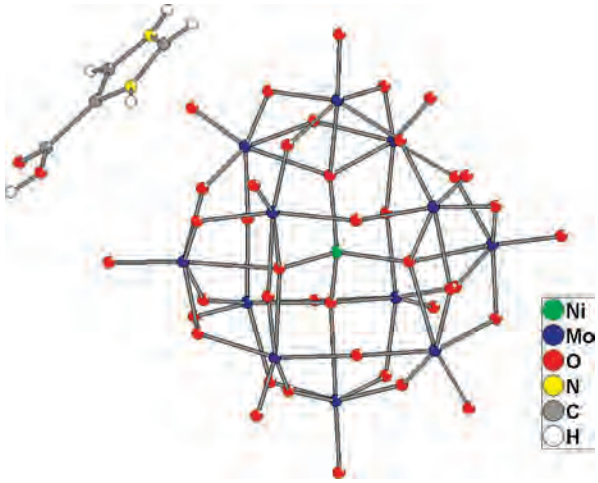

Figure 3. Ball-and-stick representation of **2** (ammonium ions are omitted).

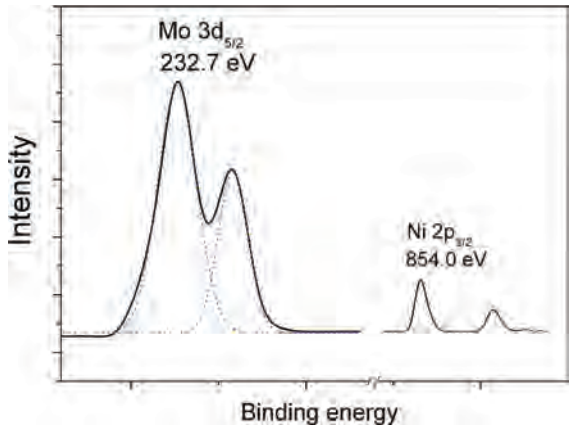

Figure 4. XPS spectra of **2** for Mo $3d_{5/2}$ and Ni $2p_{3/2}$.

to form a three-dimensional supramolecular framework as shown in Figure S7 (bottom).

Thermogravimetric Analysis (TGA). TGA was performed under N_2 at a rate of 5 °C·min^{-1} in the range of 30–800 °C on **1** and **2** (Figure S8). For **1**, a first weight loss of 7.1% occurred between 30 and 145 °C, corresponding to the loss of free water molecules (calcd 7.36%). In the range of 145–350 °C, consecutive two-step weight losses were observed with total weight loss of 17.2% corresponding to the loss of all imidazole molecules (calcd 16.95%). Then, above 650 °C, the framework of the polyoxoanion began to decompose. For **2**, a first weight loss of 2.16% occurred between 30 and 150 °C, corresponding to the loss of ammonia molecules (calcd 2.27%). In the range of 245–425 °C, the total weight loss of 19.21% corresponds to the loss of all 5-imidazolecarboxylic acid ligands (calcd 19.40%). Above 660 °C, the framework of the polyoxoanion began to decompose. All these results are in agreement with the aforementioned crystal structures.

Magnetic Properties. To confirm the CoO_4 and NiO_4 groups located in the two complexes, preliminary magnetic properties of **1** and **2** were investigated. The plots of $\chi_m T$ versus T and χ_m^{-1} versus T of **1** measured from 2 to 300 K in an applied magnetic field of 10 kOe are shown in Figure 5. The $\chi_m T$ value of **1** at 300 K is 2.34 emu·mol^{-1}·K (μ_{eff} = 4.32 μ_B), higher than the expected value μ_{eff} = 3.87 μ_B for free Co^{II} ions ($S = {}^3/_2$, g = 2.00), but in good agreement with the previously reported values that tetrahedrally coordinated Co^{2+} ion with all oxygen ligands displays a μ_{eff} value ranging from 3.94 to 4.28 μ_B.[75,76] From 300 to 120 K, the $\chi_m T$ value is almost a constant, showing a typical paramagnetic behavior. Below 120 K, the $\chi_m T$ value decreases continuously and reaches a minimum of 0.92 emu·K·mol^{-1} (2.71 μ_B) at 2 K; this behavior may result from a large zero-field splitting and spin–orbit coupling.[77,78] By Curie–Weiss law, the best linear fit of $\chi_m^{-1}(T)$ data above 120 K yields a Curie constant C = 2.55 emu·K·mol^{-1} and a Weiss constant $\theta = -15.78$ K. In addition, according to an expression of $\mu_{eff} = (8C)^{1/2}$, Curie constant C can be used to calculate μ_{eff}.[79,80] The resulting μ_{eff} = 4.51 μ_B is close to the experimental value of 4.32 μ_B, in accordance with the result of structural determination that a high spin ($S = {}^3/_2$) Co^{2+} is located in a CoO_4 coordination environment.

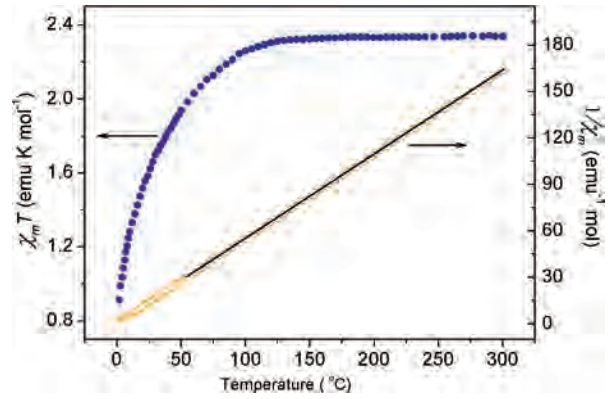

Figure 5. Plots of $\chi_m T$ versus T and χ_m^{-1} versus T from 2 to 300 K for **1** at H = 10 kOe.

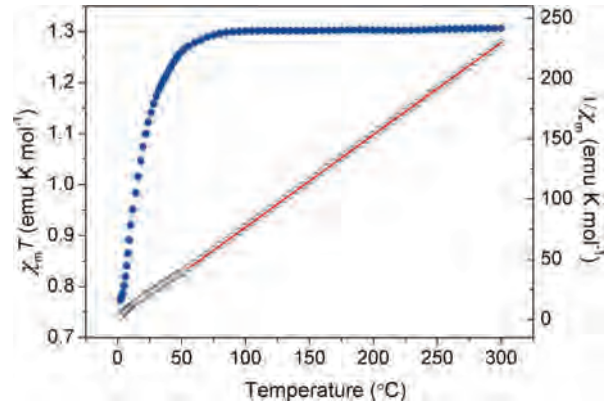

Figure 6. Plots of $\chi_m T$ versus T and χ_m^{-1} versus T from 2 to 300 K for **2** at H = 10 kOe.

As shown in Figure 6, the $\chi_m T$ value of **2** at 300 K is 1.30 emu·mol^{-1}·K (μ_{eff} = 3.22 μ_B), higher than the

(75) Cossee, P.; Van Arkel, A. E. *J. Phys. Chem. Solids* **1960**, *15*, 1–6.
(76) Dakhlaoui, A.; Ammar, S.; Smiri, L. S. *Mater. Res. Bull.* **2005**, *40*, 1270–1278.
(77) Kahn, O.; Larionova, J.; Yakhim, J. V. *Chem.—Eur. J.* **1999**, *5*, 3443–3449.
(78) Kahn, O. *Molecular Magnetism*; VCH Publishers: New York, 1993.
(79) Smart, J. S. In *Magnetism*; Rado, G. T., Shul, H., Eds.; Academic Press: New York, 1963; Vol. *3*, p 63.
(80) Zurowska, B.; Mrozinski, J.; Ciunik, Z.; Ochocki, J. *J. Mol. Struct.* **2006**, *791*, 98–105.

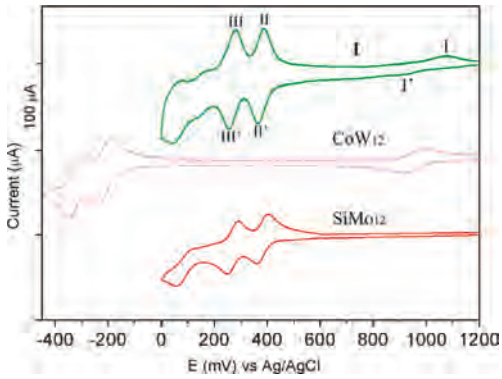

Figure 7. CV curves of 1.0×10^{-3} mol/L **1** (top), CoW_{12} (middle), and $SiMo_{12}$ (bottom) in 2 M H_2SO_4 (scan rate 50 mV/s).

expected value of $\mu_{eff} = 2.83\ \mu_B$ for free Ni^{II} ions ($S = 1$, $g = 2.00$), but in agreement with the values for tetrahedrally coordinated Ni^{2+} ion ranging from 3.1 to 4.1 μ_B.[81] From 300 to 93 K, the $\chi_m T$ value is almost a constant, also showing a typical paramagnetic behavior. Below 93 K, the $\chi_m T$ value decreases continuously to a minimum of 0.77 emu·K·mol^{-1} (2.48 μ_B) at 2 K; this behavior may result from the spin–orbit coupling. The best linear fit of $\chi_m^{-1}(T)$ data above 55 K by Curie–Weiss law yields Curie constant $C = 1.32$ emu·K·mol^{-1} and Weiss constant $\theta = -0.45$ K. The resulting $\mu_{eff} = (8C)^{1/2} = 3.25\ \mu_B$ is in agreement with the experimental value of 3.22 μ_B. These results also indicate that a high spin $S = 1$ Ni^{2+} is located in a NiO_4 coordination environment.

Electrochemical Properties. As new kinds of Keggin-type species, the electrochemical properties of **1** and **2** attract our attention because the redox properties will give us information for its further application in electrochemistry and catalysis field. Cyclic voltammetry (CV) curve of **1** consists of five redox processes in 2 M H_2SO_4 with the potential range from 1200 to 0 mV (Figure 7, top). The first process is ascribed to a Co^{3+}/Co^{2+} couple with the peak-to-peak separation, ΔE_p, of 180 mV between the reduction, E_{pc} (900 mV), and oxidation, E_{pa} (1080 mV), peak potentials (*I*′ and *I*), corresponding to the quasi-reversible redox process (ΔE_p for $Fe(CN)_6^{III}/Fe(CN)_6^{II}$ couple in this condition is 75 mV). The detailed electrochemistry data are summarized in Table 2. The redox peaks are broad and ill-defined being different than the Co^{3+}/Co^{2+} couple of CoW_{12} (Figure 7, middle) observed in the same conditions with $\Delta E_p = 73$ mV, close to the reversible one-electron redox process. When the switching potential is limited lower than 1000 mV, the Co^{3+}/Co^{2+} couple of **1** is unobserved. Such behavior is indicative of a slight electroactivity of Co^{2+} entrapped in **1**. Coulometry indicated that electron transfer per molecule for the Co^{3+}/Co^{2+} process in **1** is 0.89, similar to the value of 0.94 determined in the CoW_{12} system, which indicates that Co^{3+}/Co^{2+} couples of **1** and CoW_{12} both involve one-electron charge-transfer steps. Such behavior confirms the Co^{2+} ion being located in the polyanion of **1**, in agreement with the former crystal structure and magnetic results.

(81) Hartman, J. R.; Combariza, M. Y.; Vachet, R. W. *Inorg. Chim. Acta* **2004**, *357*, 51–58.

Table 2. Cyclic Voltammetry Data for CoW_{12}, **1**, **2**, and $SiMo_{12}$ at a Glass Carbon Electrode (Scan Rate = 50 mV/s; I_p^{Red}, I_p^{Ox} in μA; E_p^{Red}, E_p^{Ox}, ΔE_p, $E_{1/2}$ in mV)

Compound	Process	E_p^{Red}	E_p^{Ox}	ΔE_p	$E_{1/2}$	I_p^{Red}	I_p^{Red}/I_p^{Ox}
CoW_{12}	Co^{3+}/Co^{2+}	914	987	73	984.5	10.9	0.99
(in 2 *M* H_2SO_4)	W wave (1)	−235	−190	45	−212.5	21.6	1.01
	W wave (2)	−345	−301	44	−323.0	21.2	0.98
1 (in 2 M H_2SO_4)	Co^{3+}/Co^{2+}	900	1080	180	990	15.8	0.93
	Mo wave (1)	367	390	23	378.5	41.8	1.02
	Mo wave (2)	257	279	22	268	42.3	1.01
2 (pH = 0.5 H_2SO_4)	Mo wave (1)	339	363	24	351	32.6	1.17
	Mo wave (2)	214	239	25	226.5	37.2	0.99
(pH = 3.0 H_2SO_4)	Mo wave (1)	420	465	45	442.5	12.8	0.91
	Mo wave (2)	255	302	47	278.5	14.6	0.94
	Mo wave (3)	80	113	33	96.5	34.5	1.12
$SiMo_{12}$	Mo wave (1)	360	403	43	381.5	21.2	1.02
(in 2 M H_2SO_4)	Mo wave (2)	248	288	40	268.0	20.8	0.99
	Mo wave (3)	62	104	42	83.0	20.2	1.05

The second and third waves in the potential range from 500 to 200 mV are two well-defined chemically reversible couples with $\Delta E_p = 23$ and 22 mV ascribed to shell Mo centers (Table 2). The last two waves that occurred lower than 200 mV are of low current intensities and are possibly attributed to the reaction of the reduced products of processes II and III with protons from an external electrolyte, which still require further investigation. Under the same conditions, the $SiMo_{12}$ system displays three reversible redox processes with $\Delta E_p = 43$, 40, and 42 mV, respectively, over the potential range of 1200−0 mV (Figure 7, bottom). These different Mo waves belonging to **1** and $SiMo_{12}$ indicate that the central Co^{2+} ion remarkably affects the electrochemical behavior of shell Mo centers. The further electrolysis at the C electrode with couloumetric determination confirmed that the values of electron transfer per molecule for each Mo reduced process are 3.83 and 3.90 of **1**, and 1.94, 1.93, and 1.95 of $SiMo_{12}$, respectively. These data further confirm that **1** is a new kind of heteropolymolybdate showing rather unusual two four-electron reversible redox processes. By virtue of the above investigations, we can draw the following conclusions: (1) The CV behavior of **1** shows a quasi-reversible one-electron process for the Co^{3+}/Co^{2+} couple. The waves are broad, ill-defined, and even unobserved with the switching potential lower than 1000 mV. Thus, the electroactivity of Co^{2+} is lower than that of CoW_{12}. (2) The waves attributed to the shell Mo centers in **1** display consecutively two four-electron redox processes rather different to the $SiMo_{12}$ system with three two-electron redox couples. This phenomenon confirms that the Co^{2+} remarkably affects the electrochemical properties of **1**, which is probably ascribed to the distribution of the charge transfer of Co^{2+} over the whole polyoxomolybdate cluster.

The 20-cycle CV curves of **1** were conducted in the potential range from 550 to 0 mV. As shown in Figure S9, after the third cycle, the CV curves are reproducible and indicative of the stability of reversible redox processes. To the best of our knowledge, such a reversible four- to eight-electron redox system is first shown among the heteropolymolybdate compounds, which will extend the application of **1** in the electrochemical or chemical catalyst as a good multielectron reservoir. Furthermore, we also discovered that

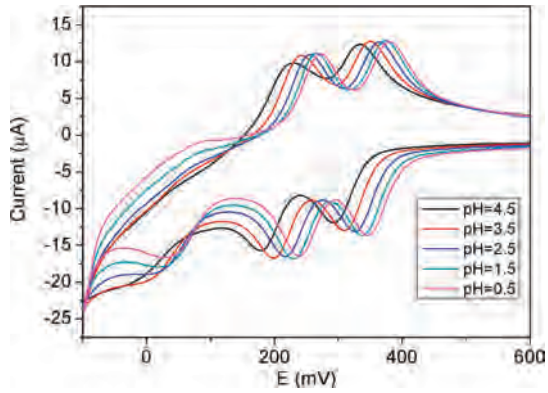

Figure 8. CV curve of 1.0×10^{-3} mol/L **1** in different H_2SO_4 solution. From left to right the pH values are 3.5, 2.5, 1.5, and 0.5, respectively; scan rate 25 mV/s.

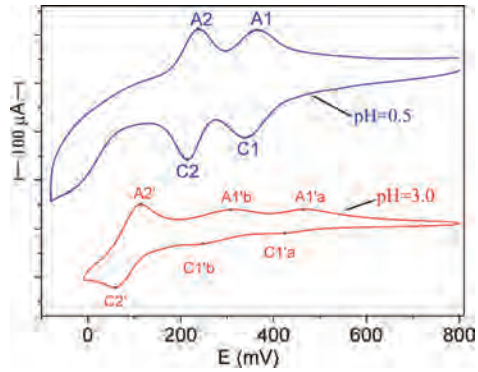

Figure 9. CV curves of 1.0×10^{-3} mol/L **2** in pH = 1.0 and pH = 3.0 H_2SO_4 solutions (scan rate 50 mV/s).

the two four-electron redox waves shift negatively in higher pH electrolytes (Figure 8). As a result, the reduced processes are strongly dependent on the combination of protons, similar to the $SiMo_{12}$ system in acidic media.[82] On the basis of the above analyses, the redox processes for Mo centers of **1** can be simply expressed as:

$$[Co^{II}Mo_{12}O_{40}]^{6-} + 4nH^+ + 4ne^- \rightleftarrows [H_{4n}Co^{II}Mo_{12}O_{40}]^{6-} \quad (n = 1, 2)$$

Because **2** shows lower solubility in pH < 0 acidic media, the electrochemical properties of **2** were investigated in pH = 0.5 and pH = 3.0 H_2SO_4 solutions. In pH = 0.5 media, no Ni^{2+}/Ni^{3+} or Ni^{2+}/Ni^{4+} redox couples were observed from 1.5 to 0.45 V, which is very different than **1** which possesses an electroactive Co^{2+} ion. However, this phenomenon is in agreement with the fact that Ni^{2+} is not an electroactive species in the POM framework.[83] Thus, all the redox waves of **2** are ascribed to the shell Mo centers. As shown in Figure 9 (top), the A1/C1 and A2/C2 couples are two well-defined chemically reversible processes with ΔE_p = 24 and 25 mV ascribed to shell Mo centers (Table 2). The couloumetric determination confirmed that the values of electron transfer per molecule for each reduced process are 3.91 and 3.95. Thus, compound **2** also shows two four-electron redox processes in pH = 0.5 H_2SO_4 solution. These two couples are similar to the observed waves in **1**, indicating the structural similarity of the two compounds. The 20-cycle CV curves of **2** were conducted in the potential range from 800 to −80 mV. As shown in Figure S10, after the second cycle, the CV curves are reproducible and indicative of the stability of redox processes.

In pH = 3.0 H_2SO_4 solution, three redox couples were observed in the potential range from 800 to −10 mV (Figure 9, bottom). The couloumetric determination indicated that the values of electron transfer for each reduced process are 1.88, 1.88, and 3.84, respectively. These values confirmed that A1′a/C1′a, A1′b/C1′b, and A2′/C2′ couples are ascribed to two two-electron and one four-electron redox processes. As a result, the A1/C1 couple is possibly ascribed to a combination of two two-electron redox processes in lower pH solution. This phenomenon is not observed for **1** even in pH = 4.5 medium. Therefore, the redox processes of complex **2** are more sensitive to the H^+ concentration of the electrolyte. The values of $E_{1/2}$ for A1′b/C1′b and A2′/C2′ shift negatively when compared to those for A1/C1 and A2/C2 couples (Table 2), suggesting that the reduced processes are also dependent on the combination of protons. So, the redox processes for **2** can be expressed as:

$$[Ni^{II}Mo_{12}O_{40}]^{6-} + 4nH^+ + 4ne^- \rightleftarrows [H_{4n}Ni^{II}Mo_{12}O_{40}]^{6-} \quad (n = 1, 2) \quad (pH = 0.5\ H_2SO_4\ \text{solution})$$

$$[Ni^{II}Mo_{12}O_{40}]^{6-} + 2H^+ + 2e^- \rightleftarrows [H_2Ni^{II}Mo_{12}O_{40}]^{6-}$$

$$[H_2Ni^{II}Mo_{12}O_{40}]^{6-} + 2H^+ + 2e^- \rightleftarrows [H_4Ni^{II}Mo_{12}O_{40}]^{6-}$$

$$[H_4Ni^{II}Mo_{12}O_{40}]^{6-} + 4H^+ + 4e^- \rightleftarrows [H_8Ni^{II}Mo_{12}O_{40}]^{6-} \quad (pH = 3.0\ H_2SO_4\ \text{solution})$$

It should be noteworthy here that complex **2** shows a more different electrochemical behavior in pH = 3.0 solution. The first two redox couples correspond to two-electron redox processes, which are unobserved for **1**. This result further confirmed that the central transition metal ion strongly affects the electrochemical behavior of the shell Mo centers.

Conclusion

By different synthetic strategies, new transition-metal-centered Keggin-type heteropolymolybdates, **1** and **2**, were isolated. The IR and UV–vis spectra of the two compounds show the characteristic bands of Keggin-type structure. Electrochemical studies of **1** demonstrate that the Co^{2+} is slightly electroactive as compared to the CoW_{12} system. The waves ascribed to shell Mo centers are consecutive two four-electron reversible processes. Compound **2** also represents two four-electron redox processes in lower pH medium. All of these four-electron processes are first observed for the heteropolymolybdate system. The significance of **1** and **2** lies in not only extending the heteropolymolybdate family as a structure point of view but also providing new promising materials as a good multielectron reservoir in the electrochemical or chemical catalysis field. The further rational syntheses of these compounds with a high yield and the exploration of their interesting physicochemical properties are in progress.

(82) Sadakane, M.; Steckhan, E. *Chem. Rev.* **1998**, *98*, 219–237.

Acknowledgment. The authors are thankful for the financial support from the National Natural Science Foundation of China (Grant Nos. 20671017 and 20731002) and the Specialized Research Fund for the Doctoral Program of Higher Education.

Supporting Information Available: X-ray crystallographic files in CIF format, IR and UV–vis spectra, three-dimensional packing figures, TGA curves, selected bond lengths (Å) and angles (°) of **1**, **2**, Mo_8Co, and Mo_7Co. This material is available free of charge via the Internet at http://pubs.acs.org.

IC700797V

(83) Timothy, M.; Bruno, F.; Gérard, B. *J. Eletroanal. Chem.* **1997**, *425*, 49–54.